2021

Extended amygdala-parabrachial circuits alter threat assessment and regulate feeding

Andrew T Luskin

Dionnet L Bhatti

Bernard Mulvey

Christian E Pedersen

Kasey S Girven

See next page for additional authors

Authors

Andrew T Luskin, Dionnet L Bhatti, Bernard Mulvey, Christian E Pedersen, Kasey S Girven, Hannah Oden-Brunson, Kate Kimbell, Taylor Blackburn, Abbie Sawyer, Robert W Gereau, Joseph D Dougherty, and Michael R Bruchas

COGNITIVE NEUROSCIENCE

Extended amygdala-parabrachial circuits alter threat assessment and regulate feeding

Andrew T. Luskin[1,2,3,4,5,6]*, Dionnet L. Bhatti[1,2]*†, Bernard Mulvey[3,7], Christian E. Pedersen[1,2,4,5,8,9], Kasey S. Girven[4,5,10], Hannah Oden-Brunson[1,2], Kate Kimbell[1,2], Taylor Blackburn[4], Abbie Sawyer[4], Robert W. Gereau IV[1,2,7], Joseph D. Dougherty[7,8], Michael R. Bruchas[1,2,3,4,5,6,7,9,10]‡

An animal's evolutionary success depends on the ability to seek and consume foods while avoiding environmental threats. However, how evolutionarily conserved threat detection circuits modulate feeding is unknown. In mammals, feeding and threat assessment are strongly influenced by the parabrachial nucleus (PBN), a structure that responds to threats and inhibits feeding. Here, we report that the PBN receives dense inputs from two discrete neuronal populations in the bed nucleus of the stria terminalis (BNST), an extended amygdala structure that encodes affective information. Using a series of complementary approaches, we identify opposing BNST-PBN circuits that modulate neuropeptide-expressing PBN neurons to control feeding and affective states. These previously unrecognized neural circuits thus serve as potential nodes of neural circuitry critical for the integration of threat information with the intrinsic drive to feed.

INTRODUCTION

All animals must successfully seek and consume food while avoiding environmental threats to survive. The internal state of an animal directly affects the expression of risky behaviors, such as exploring a dangerous environment to obtain rewards and maintain homeostasis. Animals must adaptively prioritize certain behaviors to appropriately respond to their internal state (*1*, *2*). While many studies have explored the interaction of metabolic need states with behavior, how mammals integrate affective-threat assessment with internal need states remains largely unknown.

Several recent reports have found that, in mammals, food consumption and threat assessment are heavily influenced by the parabrachial nucleus (PBN), a pontine structure that integrates visceral and sensory information to encode metabolic needs (*3*–*12*). The amygdala and extended amygdala are evolutionarily conserved brain regions that encode and integrate valence, stress, and threat to alter behavioral states. Anatomical data suggest that the PBN receives input from several regions that may encode affective information, including the bed nucleus of the stria terminalis (BNST), a structure in the extended amygdala (*8*, *13*–*15*). However, the neural circuit mechanisms that underlie the integration of an animal's own motivation to eat with internal affective states regarding environmental threats are still relatively unknown. Here, we identified two previously unknown afferents from distinct populations within the BNST to the PBN that integrate threat assessment and feeding signals to modulate PBN activity and ultimately regulate state-dependent feeding.

[1]Department of Anesthesiology, Washington University School of Medicine, St. Louis, MO 63110, USA. [2]Washington University Pain Center, Washington University School of Medicine, St. Louis, MO 63110, USA. [3]Division of Biology and Biomedical Sciences, Washington University School of Medicine, St. Louis, MO 63110, USA. [4]Department of Anesthesiology and Pain Medicine, University of Washington,

RESULTS

Anatomical and molecular characterization of opposing BNST-PBN circuits

The BNST is a heterogeneous population composed of glutamatergic, γ-aminobutyric acid (GABA)–releasing (GABAergic), and peptidergic neurons (*16*–*21*). To determine whether distinct neuronal circuits from the BNST innervate the PBN to alter feeding behaviors, we injected Cre-inducible (DIO) anterograde adeno-associated viruses (AAVs) expressing channelrhodopsin-2 (ChR2) with an enhanced yellow fluorescent protein (eYFP) reporter (AAV5-DIO-ChR2-eYFP) into the BNST of vesicular GABA transporter (vGAT)–Cre and vesicular glutamate transporter (vGLUT2)–Cre mice, which revealed robust axonal projections to the PBN from GABAergic (Fig. 1A and fig. S1, F to K) and glutamatergic (Fig. 1D) BNST neurons. To further substantiate our anterograde tracing findings, we injected retrograde AAVs (AAV2retro) expressing a Cre-inducible eYFP reporter (AAV2retro-DIO-eYFP) (*22*) into the PBN of vGAT-Cre or vGLUT2-Cre mice (fig. S1A). Retrograde tracing revealed populations of both GABAergic and glutamatergic BNST neurons that innervate the PBN (fig. S1A).

We next assessed whether these distinct populations make functional monosynaptic connections to PBN neurons using ex vivo patch-clamp electrophysiology. We collected acute brain slices containing the PBN from either vGAT-Cre or vGLUT2-Cre mice expressing DIO-ChR2-

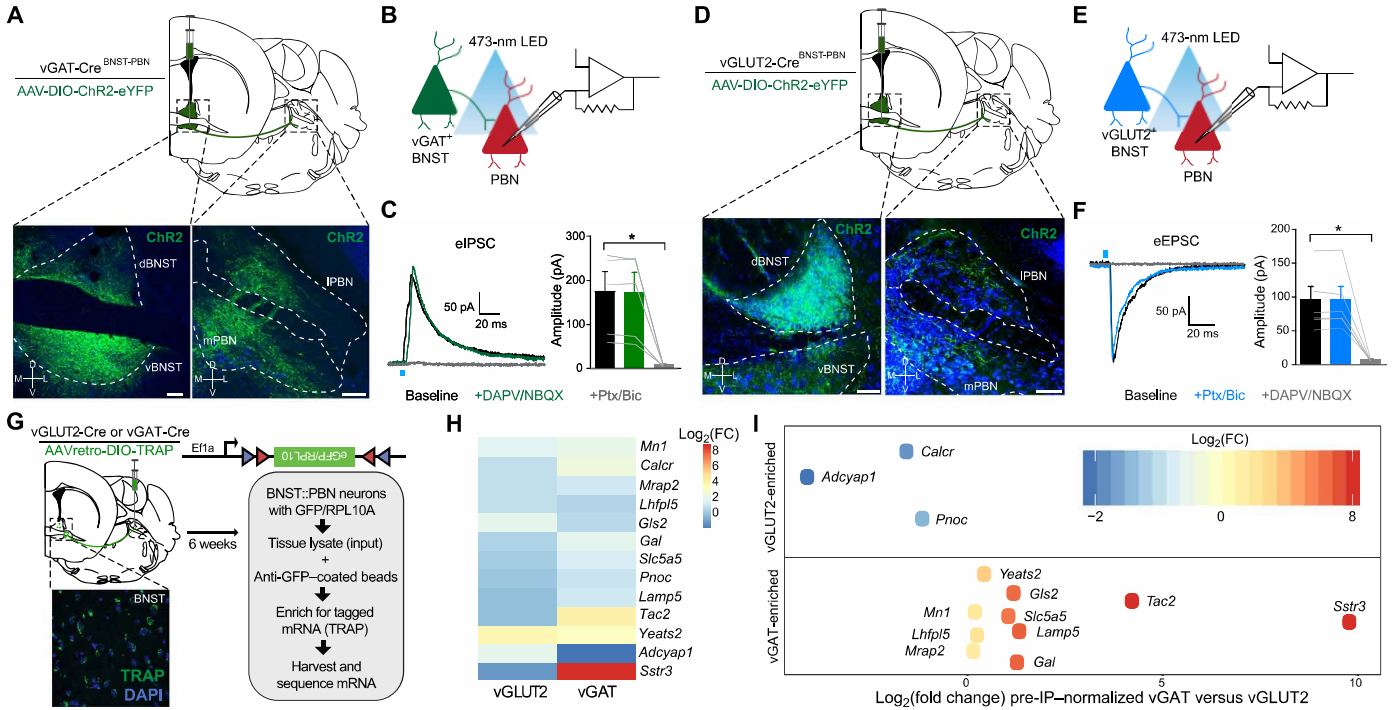

Fig. 1. Anatomical and molecular characterization of opposing BNST-PBN circuits. (**A**) Schematic of viral injection and representative image depicting expression in BNST^{vGAT} soma and their terminals in the PBN. Scale bars, 100 μm. Blue, Nissl; green, eYFP; M, medial; L, lateral; V, ventral; D, dorsal. (**B**) Schematic of whole-cell patch clamp electrophysiology recordings of optically evoked inhibitory postsynaptic currents (IPSCs). (**C**) Photoactivation of BNST^{vGAT} terminals elicits IPSCs (five of eight cells responsive) in PBN neurons that are abolished by GABA type A ($GABA_A$) receptor antagonism ($n = 5$ cells, four mice). Ptx, picrotoxin; Bic, bicuculline. (**D**) Schematic of viral injection and representative image depicting expression in BNST^{vGLUT2} soma and their terminals in the PBN. Scale bars, 100 μm. Blue, Nissl; green, eYFP. (**E**) Schematic of whole-cell patch clamp electrophysiology recordings of optically evoked excitatory postsynaptic currents (EPSCs). (**F**) Photoactivation of BNST^{vGLUT2} terminals elicits EPSCs in PBN neurons (six of nine cells responsive) that are abolished by AMPA/*N*-methyl-D-aspartate (NMDA) receptor antagonism ($n = 6$ cells, five mice). (**G**) Cartoon of injection of translating ribosome affinity purification (TRAP) into PBN of vGLUT2-Cre or vGAT-Cre animals. Tagged mRNA was extracted from the BNST and sequenced. Inset: Representative image of TRAP–green fluorescent protein (GFP) expression in BNST. (**H**) Heatmap of transcripts enriched in either vGAT or vGLUT2 projections from BNST to PBN over input homogenate [preimmunoprecipitation (pre-IP)] ($n = 3$ vGLUT2-Cre samples; $n = 2$ vGAT-Cre samples). (**I**) Transcripts enriched in either vGAT or vGLUT2 projections from BNST to PBN, after normalization to respective input (pre-IP) homogenates. Positive $\log_2$[fold change (FC)] values indicate transcript enrichment in BNST^{vGAT}-PBN neurons relative to BNST^{vGLUT2}-PBN neurons; negative $\log_2$(FC) values indicate relative enrichment in BNST^{vGLUT2}-PBN neurons. *$P < 0.05$. Error bars indicate SEM. See also figs. S1 and S2.

(Fig. 1F). Postsynaptic currents occurred <5 ms after the light pulse, suggesting that both excitatory and inhibitory connections are monosynaptic (fig. S1, B to E).

We further characterized the molecular expression profiles of these distinct inhibitory and excitatory BNST-PBN projections using translating ribosome affinity purification (TRAP) to determine their translational signature (*23*). We generated a new Cre-dependent TRAP construct within the AAV2retrovector (AAV2retro-DIO-TRAP) and injected it into the PBN of vGAT-Cre and vGLUT2-Cre mice to isolate RNA transcripts from each BNST-PBN projection population with genotype and projection specificity (*22*, *24*). We then isolated and sequenced ribosome-bound mRNA from the BNST in each group (Fig. 1G and fig. S2, A and B). The vGAT and vGLUT2 including in contexts of addiction and posttraumatic stress disorder (*32*, *33*). Both BNST^{vGAT}-PBN and BNST^{vGLUT2}-PBN neurons express calcitonin receptor (*Calcr*), recently associated with the regulation of feeding (*34*, *35*), and nociceptin (*Pnoc*), linked to motivated behaviors including feeding (*24*, *36*–*38*). We further validated these RNA sequencing (RNA-seq) findings by performing fluorescent in situ hybridization experiments, which revealed coexpression of *Tac2*, *Sstr3*, and *Calcr* with vGAT and *Adcyap1* with vGLUT2 neurons within the BNST (fig. S2, F to I).

Feeding and threat differentially engage excitatory and inhibitory BNST-PBN circuits

To determine whether these distinct genetically defined BNST-PBN

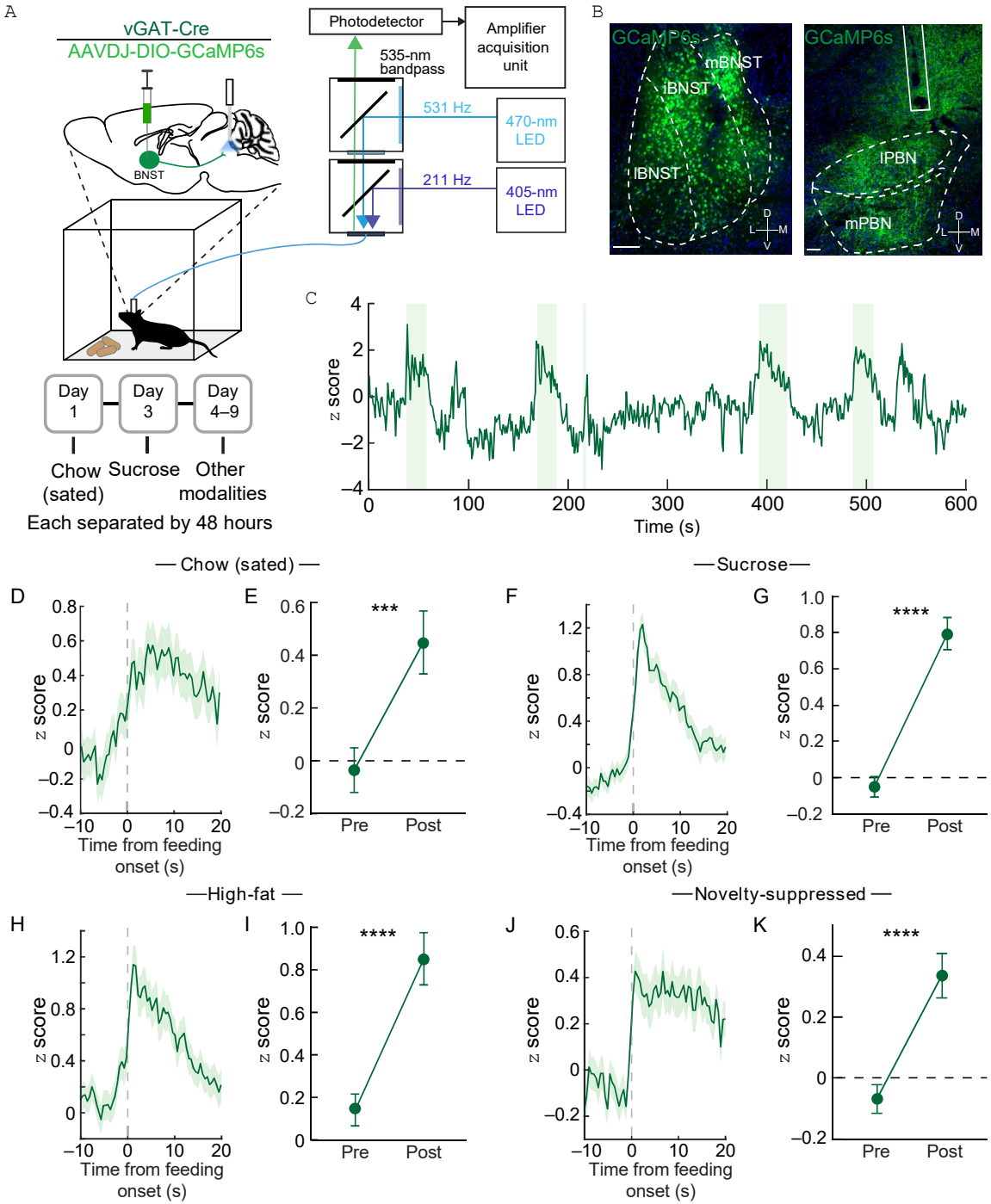

in both sated and hedonic feeding (i.e., high-sucrose chow), as well as in other food seeking modalities including high-fat, homeostatic feeding (i.e., after food deprivation), and normal chow within novel-anxiogenic environments (Fig. 2, C to K, and fig. S3G). The increase in BNST^{vGAT}-PBN activity was greater for consumption of highly palatable high-sucrose chow and lesser in a food-deprived state, compared to consumption of normal chow under a sated condition (fig. S3I). Conversely, to assess whether glutamatergic input to the PBN is altered during feeding behavior, we targeted AAVDJ-DIO-GCaMP6s to the BNST of vGLUT2-Cre mice and similarly positioned optical fibers above the PBN for measurement of BNST-PBN glutamatergic terminal calcium activity (Fig. 3, A and B, and fig. S3, B, D, and F). In these experiments, we found that, in contrast to GABAergic BNST-PBN inputs, BNST^{vGLUT2}-PBN GCaMP activity decreased when an animal engaged in these same feeding behaviors (Fig. 3, C to K, and fig. S3H). Decreases in BNST^{vGLUT2}-PBN activity

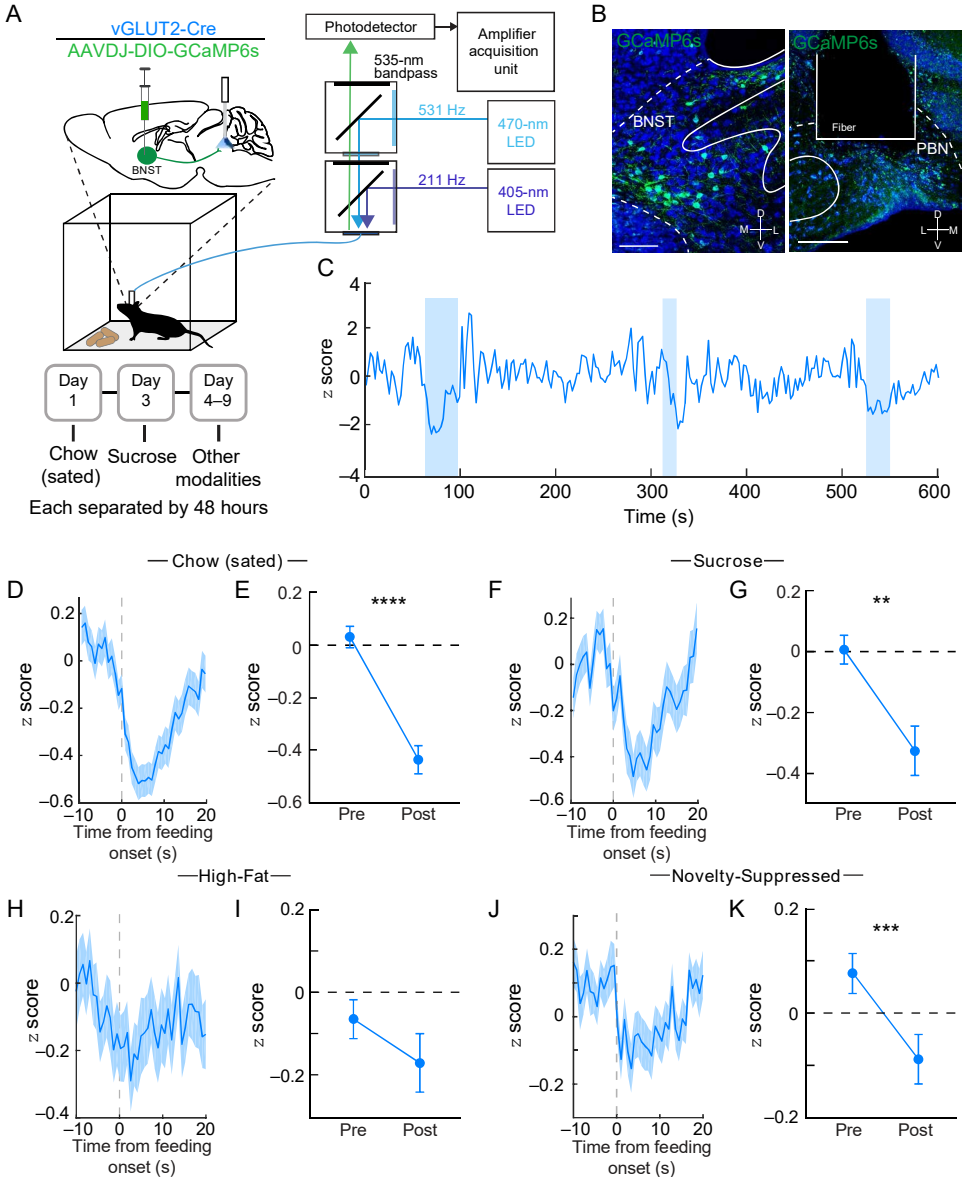

were lesser for consumption of high-fat chow and in an anxiogenic environment, relative to normal sated chow consumption (fig. S3J). To evaluate whether these changes in activity were due simply to food presence or approach, we assessed calcium activity, while animals attempted to eat an inaccessible food item (fig. S3, U and V). Our findings demonstrate that the change in either vGAT or vGLUT2 BNST-PBN terminal activity is not associated with the approach or presence of food. When animals attempted to eat a false food item, however, we found a subtle but stable increase in $BNST^{vGAT}$-PBN GCaMP fluorescence (fig. S3W), consistent with the notion that this circuit is involved in food consumption. Alternatively, we observed no change in $BNST^{vGLUT2}$-PBN GCaMP fluorescence when animals attempted to consume false food (fig. S3X). Furthermore, neither vGAT nor vGLUT2 BNST-PBN terminals exhibited an increase in GCaMP activity when interacting with a novel or familiar object (fig. S3, Y to BB). Together, these data further support opposing roles for GABAergic and glutamatergic BNST-PBN circuits in modulating consummatory feeding behavior.

Food seeking requires an integration of threat assessment and anxiety-like behavior to adaptively seek out and consume food, as it is necessary for survival. We therefore hypothesized that if these circuits alter feeding behavior concurrently with threat assessment, then GABAergic or glutamatergic BNST-PBN input may be differentially engaged during aversive threat stimuli. To assess this, we recorded from BNST-PBN terminals in vGAT-Cre and vGLUT2-Cre mice during the presentation of multiple shock stimuli (Fig. 4A). When animals were presented with an aversive shock, $BNST^{vGAT}$-PBN GCaMP activity rapidly decreased in response (Fig. 4, B to D), while $BNST^{vGLUT2}$-PBN GCaMP activity increased following shock (Fig. 4, E to G). Similarly, $BNST^{vGAT}$-PBN calcium activity decreases (Fig. 4, H to J), whereas $BNST^{vGLUT2}$-PBN calcium activity increases (Fig. 4, K to M), upon entry into an innately anxiogenic environment such as the open arms of an elevated zero maze (EZM). Unexpectedly, no change in terminal activity in either projection arose after tone-shock associations were made and shock-predictive cues were presented alone (fig. S3, CC and DD). These observations indicate that inhibitory GABAergic BNST-PBN circuits may act to diminish threat signaling to engage and allow feeding, while excitatory glutamatergic BNST-PBN circuits are likely recruited to enhance threat signaling and suppress feeding behaviors in response to immediately threatening stimuli.

Excitatory and inhibitory BNST-PBN circuit activation induce opposing feeding behaviors

Because photometry measurements at BNST-PBN terminals revealed that these two opposing BNST-PBN projections are modulated during feeding and threat responses, we next used optogenetic approaches to assessing whether manipulating neural circuit activity of BNST-PBN circuits alters feeding, threat, and affective valence and to determine direct causality of this circuit in regulating behavior.

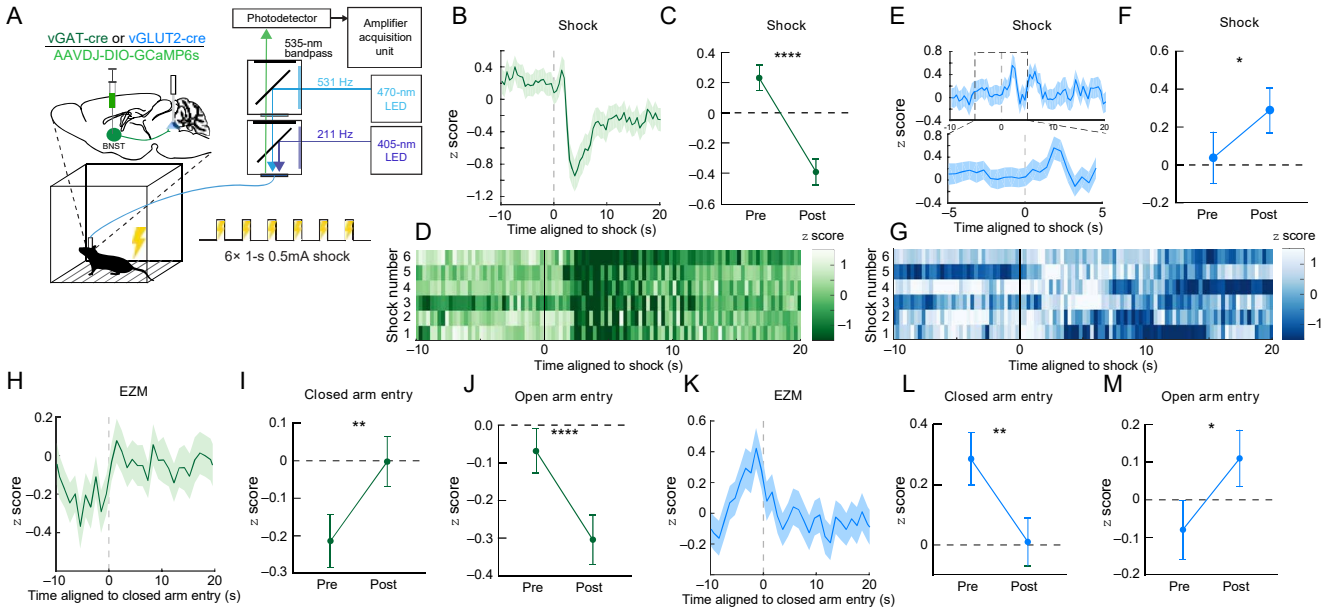

Fig. 4. Distinct BNST-PBN circuits display opposing responses to aversive stimuli. (**A**) Schematic of in vivo fiber photometry and behavior. (**B**) Average *z*-scored calcium transient responses of $BNST^{vGAT}$-PBN terminals to an aversive shock ($n = 7$ mice). (**C**) Mean *z*-scored calcium transient responses of $BNST^{vGAT}$-PBN terminals ($n = 7$

We targeted AAV5-EF1α-DIO-ChR2 to the BNST of vGAT-Cre or vGLUT2-Cre mice and positioned optical fibers above the PBN for photostimulation of BNST-PBN GABAergic or glutamatergic terminals (Fig. 5A). First, we measured food consumption with or without genetically defined neural circuit photoactivation, while mice had free access to different foods (Fig. 5B). Neurons were photostimulated at 20 Hz, consistent with previously identified firing rates in BNST projection neurons (*20*). First, to ensure that a homeostatic drive to feed was elicited by withdrawal of food, we measured food consumption under sated and food-deprived conditions (Fig. 5C). Activation of ChR2 in BNST^{vGAT}-PBN neurons increased food consumption compared to control mice under sated conditions (Fig. 5D and fig. S4A). This increase also occurred with sucrose and high-fat foods (fig. S4, C to E). No change, however, was observed when mice were in a food-deprived state (Fig. 5D and fig. S4B), suggesting that inhibitory BNST-PBN circuits are already engaged, consistent with our fiber photometry results (fig. S3G). Furthermore, photoactivation of BNST^{vGAT}-PBN signaling also increased consumption of less-palatable salt-enriched or bitter (i.e., quinine-enriched) foods (fig. S4, F to H). Moreover, BNST^{vGAT}-PBN activation is sufficient to drive animals to attempt to consume non-food items (fig. S4J). Together, these results suggest that the inhibitory BNST-PBN circuit is sufficient to drive feeding in sated states, regardless of taste modality or caloric content. In contrast to activation of BNST^{vGAT}-PBN, activation of BNST^{vGLUT2}-PBN in a food-deprived state decreased the consumption of normal chow (Fig. 5D and fig. S4, W and X), demonstrating that the excitatory BNST-PBN circuit is sufficient to reduce feeding when mice are in a food-deprived state. Photostimulation of either inhibitory or excitatory BNST-PBN circuitry did not change body temperature (fig. S4O), suggesting that the effects on feeding are independent of thermoregulation, an identified role of PBN neurons (*41*).

We next sought to determine the necessity of BNST-PBN circuits for feeding behavior. We performed projection-specific chemogenetic inhibition experiments by injecting an AAV5-DIO-hM4Di-DREADD (*42*) in the BNST of vGAT and vGLUT2-Cre mice and infusing clozapine N-oxide (CNO) into the PBN through a cannula (Fig. 5Q). We found that, in a sated state, inhibition of BNST^{vGLUT2}-PBN projections increased feeding compared to inhibition of BNST^{vGAT}-PBN projections (Fig. 5R). When animals were fasted for 24 hours, inhibition of BNST^{vGAT}-PBN projections decreased feeding relative to inhibition of BNST^{vGLUT2}-PBN neurons and control mice (Fig. 5S). These findings were also corroborated with photoinhibition of the BNST^{vGAT}-PBN circuit using Arch3.0 (fig. S4, S and T). Together, these results indicate that binary and opposing BNST-PBN circuits bidirectionally modulate food consumption.

Excitatory and inhibitory BNST-PBN circuit activation induce opposing affective states

Internal states and affective valence alter an animal's ability to assess potential threats and explore different environments, a re-

resulted in a robust place preference for the photostimulation-paired side, while photoactivation of ChR2 in BNST^{vGLUT2}-PBN neurons resulted in a robust place aversion for the photostimulation-paired side, as compared to controls (Fig. 5, E and F). In an operant self-stimulation paradigm (Fig. 5G), photoactivation of BNST^{vGAT}-PBN neurons significantly increased the number of nose pokes for self-stimulation relative to controls (Fig. 5H), demonstrating that BNST^{vGAT}-PBN stimulation is positively reinforcing. Conversely, photoactivation of BNST^{vGLUT2}-PBN neurons significantly increased the number of nose pokes mice performed to turn off photostimulation (Fig. 5I and fig. S4Y), demonstrating that BNST^{vGLUT2}-PBN stimulation is negatively reinforcing. These data indicate that activation of GABAergic and glutamatergic BNST-PBN circuits have innate positive and negative affective valence, respectively (*46*).

To determine whether BNST-PBN circuits modulate threat assessment, we tested mice in the EZM, which measures anxiety-like behaviors and exploration in a novel anxiogenic context (*43*). Photoactivation of BNST^{vGAT}-PBN induced an anxiolytic-like state characterized by more time spent in the open arms compared to controls (Fig. 5J and fig. S4K), consistent with increased exploratory drive. In contrast, photoactivation of BNST^{vGLUT2}-PBN neurons induced an anxiogenic-like state characterized by less time spent in the open arms (Fig. 5K), indicating that stimulation of this circuit is sufficient to reduce exploration of an anxiogenic environment. As a further test of whether BNST^{vGAT}-PBN activation can suppress defensive behaviors associated with threat, we subjected mice to threat conditioning and measured their defensive response (i.e., freezing) to a conditioned stimulus. Mice were trained to associate a conditioned stimulus (tone) with a highly aversive unconditioned stimulus (0.7 mA, 2-s foot shock). Photostimulation of BNST^{vGAT}-PBN neurons robustly reduced the defensive responses to the conditioned stimulus, likely through overriding threat responses and driving exploration associated with food seeking (Fig. 5, L and M). Photoactivation did not alter extinction retention, suggesting that BNST^{vGAT}-PBN activity may simply reduce threat responsivity. To test whether suppression of these circuits could modulate affective behaviors, we tested whether chemogenetic inhibition of BNST-PBN terminals could alter exploration in the EZM. Inhibition of BNST^{vGAT}-PBN neurons decreased exploration in an EZM (Fig. 5T). These data indicate that BNST-PBN circuits are necessary and sufficient for regulating opposing threat- and anxiety-related behavioral states.

To determine whether BNST-PBN circuitry modulates feeding in a threatening context, we performed conflict feeding assays, which pit the drive to feed against its urge to explore a novel anxiogenic environment. While stimulation of BNST^{vGLUT2}-PBN neurons decreased feeding and increased the latency to feed in under anxiogenic conditions in the open-field test (OFT), stimulation of BNST^{vGAT}-PBN neurons increased feeding (Fig. 5, N and O). Stimulation of BNST^{vGAT}-

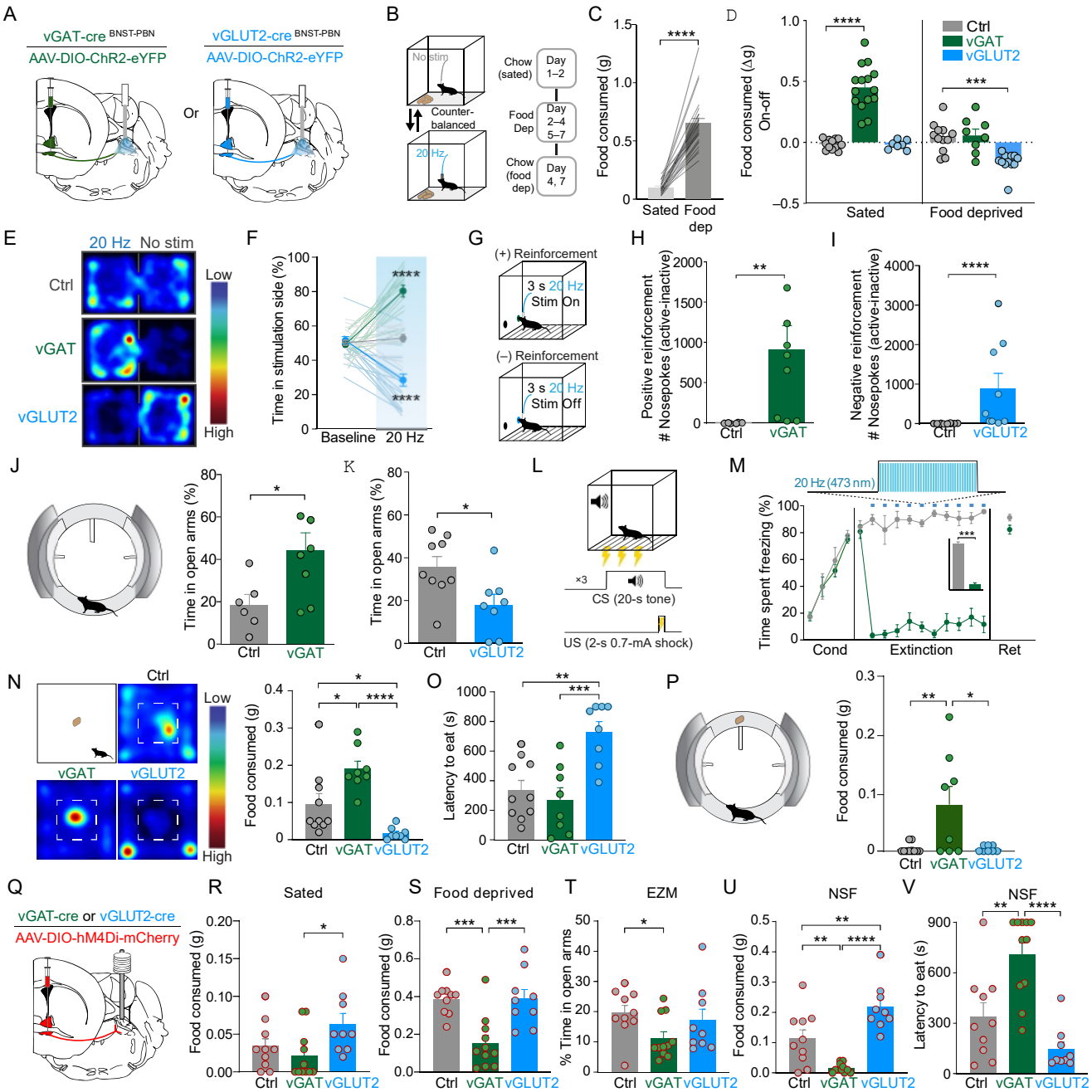

Fig. 5. Distinct BNST-PBN circuits drive opposing feeding and affective behaviors. (**A**) Schematic of optogenetic approach to targeting BNST^{vGAT}-PBN and BNST^{vGLUT2}-PBN. (**B**) Schematic of food consumption assay. (**C**) Food deprivation increases food consumption in control animals. (**D**) BNST^{vGAT}-PBN activation increases consumption of normal chow under sated conditions, whereas BNST^{vGLUT2}-PBN activation decreases consumption of normal chow after food deprivation. (**E**) Representative heatmaps of time spent in the real-time place preference (RTPP) for Ctrl, BNST^{vGAT}-PBN:ChR2, and BNST^{vGLUT2}-PBN:ChR2 mice. (**F**) BNST^{vGAT}-PBN activation elicits an RTPP, while BNST^{vGLUT2}-PBN activation elicits a real-time place aversion, compared to control mice. (**G**) Schematic of positive (BNST^{vGAT}-PBN:ChR2) and negative (BNST^{vGLUT2}-

Excitatory and inhibitory BNST afferents target both dynorphin and calcitonin gene-related peptide neurons in PBN

We next aimed to determine the specific targets of $BNST^{vGAT}$ and $BNST^{vGLUT2}$ projections in the PBN. Previous studies have identified diverse neuronal populations within the primarily glutamatergic PBN (*4*, *10*, *47*, *48*). The PBN contains multiple neuropeptidergic populations, including neurons that synthesize and release calcitonin gene-related peptide (CGRP) (*4*) and dynorphin (pDyn) (*47*). To further explore how PBN neurons downstream of BNST-PBN circuits regulate feeding and affective behaviors, we examined the organization of PBN dynorphin (pDyn) neurons, previously shown to regulate thermoregulation (*47*, *49*) and ingestion in response to mechanosensory feedback (*12*), and CGRP neurons (*4*–*6*), shown to function as a general alarm system that responds to threats and inhibits feeding when activated. In situ hybridization experiments demonstrated that pDyn neurons (PBN^{pDyn}) and CGRP neurons (PBN^{CGRP}) form genetically and anatomically distinct populations in the PBN (Fig. 6, A and B). We determined which of these populations received input from BNST projections by expressing ChR2 under a CAG promoter in BNST neurons and recording from parabrachial neurons labeled by crossing Calca (calcitonin related polypeptide alpha)-Cre mice with the fluorescent reporter line Ai14 or by injecting AAV-DIO-mCherry into the PBN of pDyn-Cre mice (Fig. 6C). We performed ChR2-assisted circuit mapping via whole-cell patch clamp recording of these genetically defined PBN neurons while photoactivating BNST terminals expressing ChR2 (*50*). Photostimulation of BNST terminals in the PBN elicited eIPSCs and eEPSCs that were abolished with bath application of tetrodotoxin (TTX) and then restored with 4-aminopyridine (4-AP) demonstrating the BNST forms monosynaptic connections with pDyn- and Calca-expressing PBN neurons (Fig. 6, D and G). We also found that photostimulation of BNST terminals evoked small EPSCs in separate pDyn and CGRP neurons that were blocked with TTX and could not be restored with application of 4-AP, indicating polysynaptic connections (Fig. 6, E and H). pDyn- and CGRP-expressing PBN neurons receive distinct proportions of excitatory and inhibitory BNST input. About 62% of PBN^{pDyn} neurons receiving monosynaptic connections from the BNST received both eIPSCs and eEPSCs, while the remaining 38% received only eEPSCs (Fig. 6I). In contrast, about 83% of PBN^{CGRP} neurons received both eIPSCs and eEPSCs, whereas the remaining 17% received only eIPSCs (Fig. 6J). Furthermore, using transynaptic rabies tracing (*51*–*53*), we found that BNST neurons form monosynaptic connections with pDyn-expressing neurons in the PBN (fig. S5, A to C). These data reveal that both inhibitory and excitatory BNST-PBN circuits modulate the activity of both pDyn- and Calca-expressing PBN neurons. These data position both PBN^{CGRP} and PBN^{pDyn} as critical downstream nodes for the behavioral effects of inhibitory and excitatory BNST-PBN inputs. Nonetheless, how PBN^{pDyn} modulates affective-feeding behaviors has not been thoroughly investigated.

an anxiogenic open field (Fig. 7C). Furthermore, shock elicited rapid activation of PBN^{pDyn} activity, which was followed by a decrease (Fig. 7D). PBN^{pDyn} neurons decreased activity in response to a conditioned threat-predictive cue (fig. S5, D and E) and upon entry into the open arms of EZM (Fig. 7E), suggesting that the activity of this neuronal population may increase to immediately aversive events but be suppressed when threats are unclear or less imminent. PBN^{pDyn} activity did not change when animals chewed a false food pellet, sniffed inaccessible food, or interacted with a novel or familiar object (fig. S5, F to I). Together, these data support the conclusion that PBN^{pDyn} neurons are engaged during feeding and disengaged when exploring anxiogenic environments.

To further assess whether PBN^{pDyn} activation is sufficient to alter feeding and affective behaviors, we targeted dynorphin-expressing PBN neurons in pDyn-Cre mice with AAV5-EF1α-DIO-ChR2 and subjected the mice to both feeding and affective behavioral tests (Fig. 7, F and G). Consistent with the effects of excitatory BNST-PBN activation, we found that photostimulation of PBN^{pDyn} produces a robust real-time place aversion (Fig. 7, H to J, and fig. S5K) and reduced feeding when animals were in a food-deprived state (Fig. 7K and fig. S5L). In addition, inhibition of the broader glutamatergic PBN population rapidly and reversibly increased food consumption (fig. S5, M and N). Likewise, chemogenetic inhibition of PBN^{pDyn} neurons using the hM4Di DREADD strategy (Fig. 7, L and M) (*42*) decreased the latency to consume food in an anxiogenic environment and increased overall food consumption in mice expressing the inhibitory DREADD when given CNO compared to saline, while control animals did not differ between treatments (Fig. 7, N to P). Consistent with this finding, the inhibition of PBN^{pDyn} neurons produced and anxiolytic-like state in the EZM test after CNO treatment (Fig. 7Q and fig. S5, O and P). These data reveal a complex, previously unrecognized functional role of PBN^{pDyn} neurons as important integrators of BNST afferents, likely alongside PBN^{CGRP} neurons, that contribute to coordinating feeding drive, together with peripheral threat and affective information.

DISCUSSION

These studies indicate that discrete, neuropeptide-expressing, opposing neural circuitry from the BNST to the PBN modulates affective valence, threat assessment, and feeding behavior. The BNST has been shown to be involved in numerous functions related to threats and motivated behaviors (*54*), and our findings demonstrate that the BNST conveys sensory and affective information to two key neuropeptide containing populations (pDyn and Calca) in the PBN to alter behavior critical to an animal's survival.

Recent studies have demonstrated BNST input to the PBN and revealed that BNST neurons may influence respiration and anxiety via increased metabolic activity in the PBN (*13*, *15*). However, studies to date had not determined the identity of these projections.

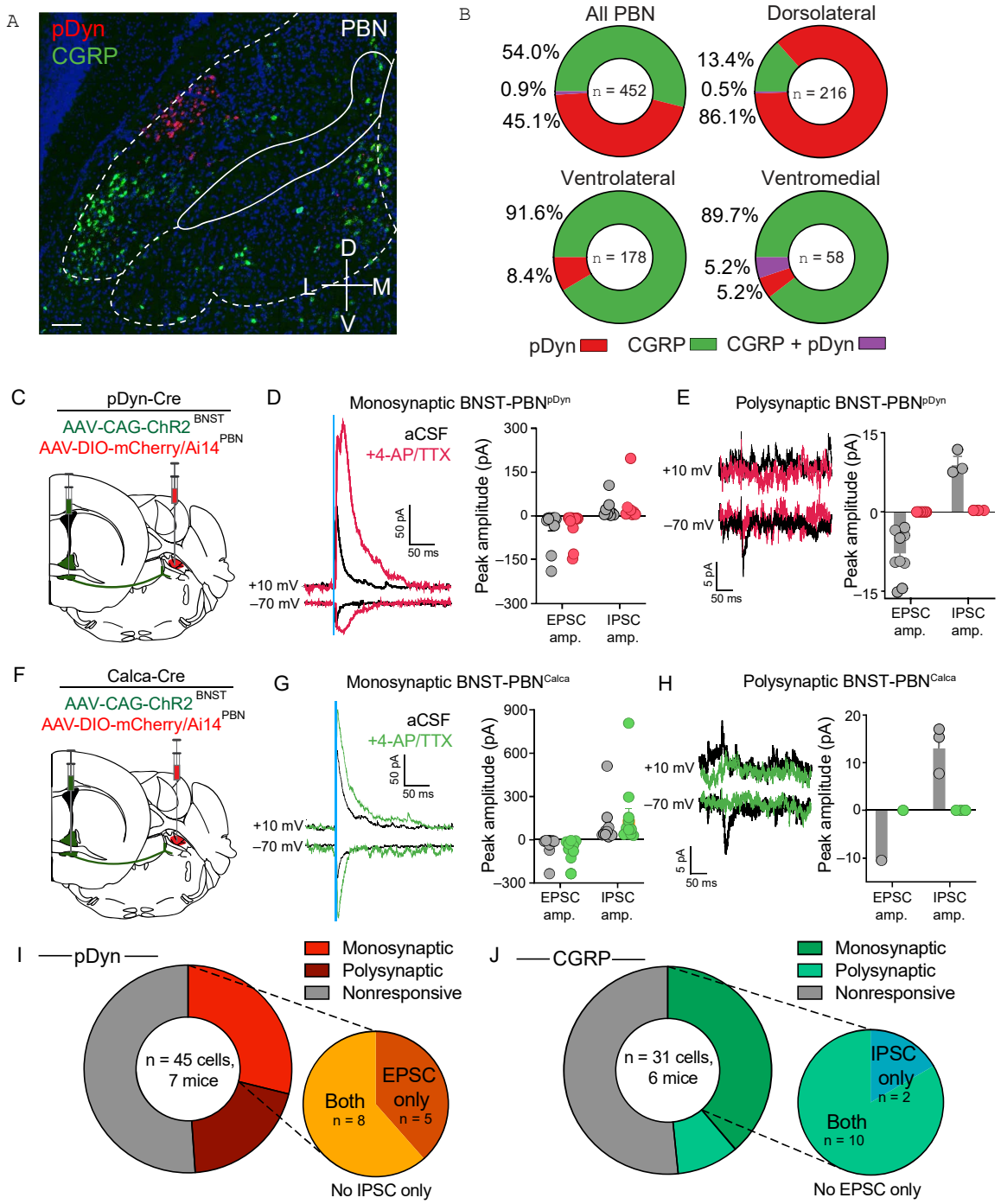

Fig. 6. Dynorphin- and CGRP-expressing PBN neurons receive both excitatory and inhibitory BNST input. (**A**) Fluorescent in situ hybridization of pDyn and CGRP in the PBN. Scale bar, 100 μm. (**B**) pDyn and CGRP neurons are genetically and anatomically distinct populations in the PBN ($n = 452$ cells). Plots represent the percentage of